Article

a special issue for the scientific conference held by the Department of Chemistry- College of Education for Girls/University of Kufa and in cooperation with Hilla University College, under the title (**5'th Postgraduate Students Annual Conference**) **(PSAC2024)**, which held for Wednesday, **24/4/2024.**

Development and Analysis of Inorganic Perovskite material for Solar Cells

Hala Allawi Kadhum and Majida Hameed Khazaal

Department of Chemistry/ Faculty of Education for Girls/ Kufa University/ Iraq

halaa.altaai@student.uokufa.edu majidah.alkhazaali@uokufa.edu

Abstract

In this work, for the first time a blend of a prepared nano barium titanate $BaTiO_3$ using hydrothermal method and $Cs_3Bi_2I_9$ was used as a perovskite material for photo anode layer fabrication to be used in photovoltaic pv solar cell. This prepared layer was characterized through XRD, SEM and UV-Vis spectroscopy and the findings state that the band gap of the prepared layer was reduced further compared to the original material of barium titanate (insulating material) suggesting that the prepared material is promising in the PV cell. This fact was further confirmed through performance testing, which showed that the Insulating short circuit current (Isc) measured 5 mA and the photoconversion efficiency (PCE) was 2.4%. It was found the morphology of the prepared layer was also improved.

Key words; Perovskite, Barium titanate, PV cell, and Hydrothermal

1. Introduction

In the modern century, the problem of energy sources is one of the first issues that researchers try to delve into, considering reducing pollution resulting from energy sources. Hence, renewable energy, particularly solar energy, is the most suitable choice for fulfilling the global energy requirements. Solar energy is distinguished by its availability as a clean energy source that can be effortlessly turned into electricity [1].

The most common type of solar cell is a PN junction, which uses the photovoltaic effect to generate electricity when light hits it. In this junction type, the N-type semiconductor area faces the light source as shown in figure 1. (a, b), the semiconductor material absorbs incident photons with energies equal to its energy gap, creating electrons, and holes as charge carriers. A voltage is produced as a result of the separation of these electrons and holes caused by the inherent potential [2]. The fundamental attributes of a solar cell include the short circuit current (I_{SC}), open circuit voltage (Voc), Fill Factor (FF), and solar energy conversion efficiency (η). Figure (1-b) displays many types of solar cells [3]. Perovskite Solar cells have shown substantial advancements in recent years compared to other photovoltaic (PV) technologies. Organic-inorganic hybrid perovskite (OIHP) is a type of perovskite photovoltaic cell (PSC) with a structure represented as ABX_3. In this structure, A represents a monovalent ion, B represents a divalent ion, and X represents a halogen ion or oxygen ion [4]. These materials have gained prominence because of their exceptional optical and electrical qualities, as well as their simplicity and affordability. The efficiency of (PCE) for photoelectric conversion of PSCs has experienced a significant and rapid improvement, going from an initial value of 3.8% to a certified value of 25.5% in only ten years [5]. In recent times, there has been a significant amount of research focused on $CH_3NH_3PbI_3$ based perovskite photoelectric cells. This is due to its exceptional ability to convert sunlight into electricity and its straightforward manufacturing procedure [6]. Due to its toxicity, researchers have attempted to replace lead (Pb) in perovskite structures with tin (Sn) and

germanium (Ge), both of which belong to group-14 metals. While Sn^{+2} and Ge^{+2} can replace Pb to form a less toxic perovskite structure, they are not as stable as Pb^{+2} when exposed to air. As a result, there has been recent interest in Bi-based halide perovskites with the chemical formula $A_3Bi_2X_9$ (where A represents a monovalent cation such as Na^+, K^+, Rb^+, Cs^+), as they offer a solution to the stability and toxicity issues associated with lead-based perovskite materials [7]. Advancements in nanotechnology have led to significant progress in various areas, including solar cell technology. Researchers have successfully incorporated nanoparticles into solar cells, enhancing their energy transfer efficiency. This breakthrough holds promise for sustainable energy solutions, as nanoparticles effectively mitigate static electricity caused by the ionic charge on the polar surface [8]. Barium titanate ($BaTiO_3$) is a ceramic material with ferroelectric properties, making it an excellent electrical insulator. Nevertheless, with the addition of trace amounts of metals, particularly scandium, yttrium, neodymium, cesium, and others, its properties shift to those of a semiconductor [9]. Ferroelectric substances are incorporated into the PSCs to modify the residual polarization electric field utilising an external electric field, thereby controlling the movement of ions and carriers [5].

For this study, a nano-inorganic ferroelectric material called BaTiO3 has been synthesized. This material exhibits a strong spontaneous polarization and possesses a structure like that of the perovskite film. Subsequently, the composite optical absorption layer was fabricated utilizing the aforementioned material. Afterward, the nanostructures and chemical compositions were analyzed using XRD, SEM, and UV-spectroscopy. Additionally, the photoelectric running of the perovskite solar cells (PSCs) was measured.

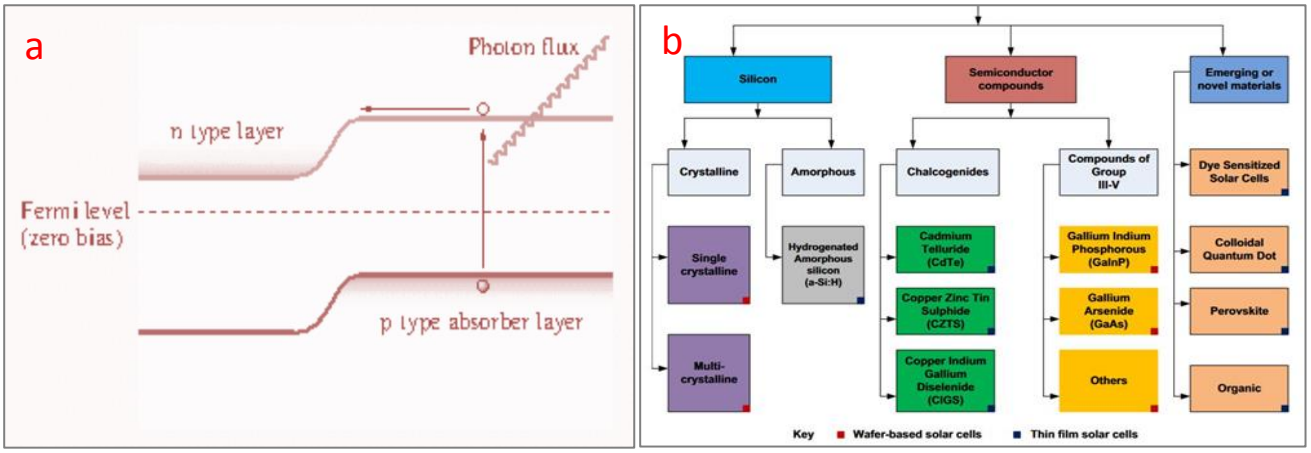

Figure1.(a)PN junction demonstrates the absorption of incident photons, the generation of electrons and holes, and the diffusion of electrons towards the junction [10]**, (b) Classification of solar cells based on the primary active material they utilize** [3]**.**

2. Experimental

2.1. Synthesis of $BaTiO_3$ perovskite nanoparticles

The BaTiO3 perovskite was synthesised using a hydrothermal technique. Barium hydroxide octahydrate crystals were combined with titanium dioxide powder at a ratio of Ba/Ti = 1.64. Then, a 30 mL solution of ammonia (10 M) was added to the mixture and stirred for a duration of 15 minutes. The solution was moved to a 50 mL autoclave bottle made of stainless steel and lined with Teflon. The hydrothermal reactions were conducted at 130 °C for 72 h. After the completion of the reaction, the container was allowed to cool down to the surrounding temperature. The resultant compounds were isolated and purified by washing with ethanol, followed by multiple washes with distilled water. The purified products were then dried in an oven at a temperature of 60 ℃ for 24 hours.[11]. The production of barium titanate is a simple procedure when titanium dioxide and barium hydroxide are employed, as demonstrated in Equation 1.

$$TiO_2 + Ba(OH)_2 \longrightarrow BaTiO_3 + H_2O \quad \ldots\ldots(1)$$

2.2. Synthesis of $BaTiO_3$/ $Cs_3Bi_2I_9$

Initially, a 10 mL solution containing a mixture of DMF and DMSO in a volume ratio of 3:1 was made and transferred to bottle (A) for later use. 0.13 mg of $BaTiO_3$ particles were precisely measured and placed into bottle B. Then, the combined solution from bottle (A), which had a volume of 3.3 ml, was poured into bottle (B). The precursor solutions would be agitated until the powders were uniformly distributed throughout the solution. Afterward, a 5 mL solution containing a mixture of DMF and DMSO was drawn into bottle (C). Next, a solution containing $Cs_3Bi_2I_9$ was prepared by combining 0.6488 g of CsI powder with 4 ml of hydroiodic acid and 5 ml of anhydrous dimethylformamide (DMF). Subsequently, a quantity of 1 g of powdered BiI_3 was completely dissolved in 5 ml of DMF. Subsequently, the two solutions were amalgamated in a beaker while being agitated incessantly at a temperature of 50 ℃ [12]. As in the following equation:

$3CsI+2BiI_3 \longrightarrow Cs_3Bi_2I_9$ …….. (2) .

precursor solution included 1.33 ml solution of bottle B and 1.33 ml solution of bottle C. The precursor solutions will be agitated at a temperature of 60 ℃. to get $BaTiO_3$/$Cs_3Bi_2I_9$ for use in device fabrication [5]**.**

2.3. Synthesis CuO nanoparticles

A copper powder sample (Cu powder, Ranbaxy) with a diameter greater than 5 μm was utilised as a copper source. The powder was subjected to a cleaning process involving ultrasonic treatment in both acetone and water solvents for 10 minutes in each solvent. For preparation, Teflon-lined stainless steel was utilised. In a glass vial, 2 mg of copper powder was mixed with 20 ml of deionized water. To prevent the mixture from clumping together, a small amount of ethylenediamine (en) was added to the reaction mixture. After subjecting the reaction mixture to sonication for approximately 30 minutes in a glass veil, it was moved into a 100 ml metallic bomb lined with stainless steel Teflon and sealed under standard circumstances. After that, the sealed container was set into a preheated box furnace, and the contents were gradually heated to 180 degrees Celsius (2 degrees Celsius per minute) and

kept there for twelve hours. Once the specified duration has elapsed, we cool the furnace. Centrifugation extracts the product from the ensuing suspension. Following this, the product is washed and dried for a few hours [13]. as denoted in the following equations (3 and 4).

$$Cu_2 + 2OH^- \rightarrow Cu(OH)_{2\,(S)} \ldots\ldots\ldots(3)$$

$$Cu(OH)_{2(S)} \xrightarrow{\Delta} 2CuO_{(S)} + 2H_2O_{(l)} \ldots\ldots\ldots(4)$$

2.4. Fabrication of devices

The ITO conductive glasses were cleaned and then coated with a compact layer solution of TiO_2 using a drip coating method (ETM). The precursor was formed by diluting a TiO_2 slurry with alcohol at a ratio of 1:7 and thereafter subjecting it to a treatment at a temperature of 500 ℃ for 30 minutes. The $BaTiO_3/Cs_3Bi_2I_9$ compound was applied to the modified layer's surface using a drip coating method. A volume of 250 mL of chlorobenzene was carefully applied to the film. Subsequently, the annealing process was conducted on the heating platform in two stages (60 ℃, 2 min; 120 ℃, 10 min) [14, 15]. Finally, 3 mg of CuO nanocomposite with 1 ml of chlorobenzene was mixed to form the p-type HTM composite by drip-coating.[16]. The counter electrodes on the Al- electrodes were made of 1 cm^2 of Al foil.[12], as shown in figure 2.a.

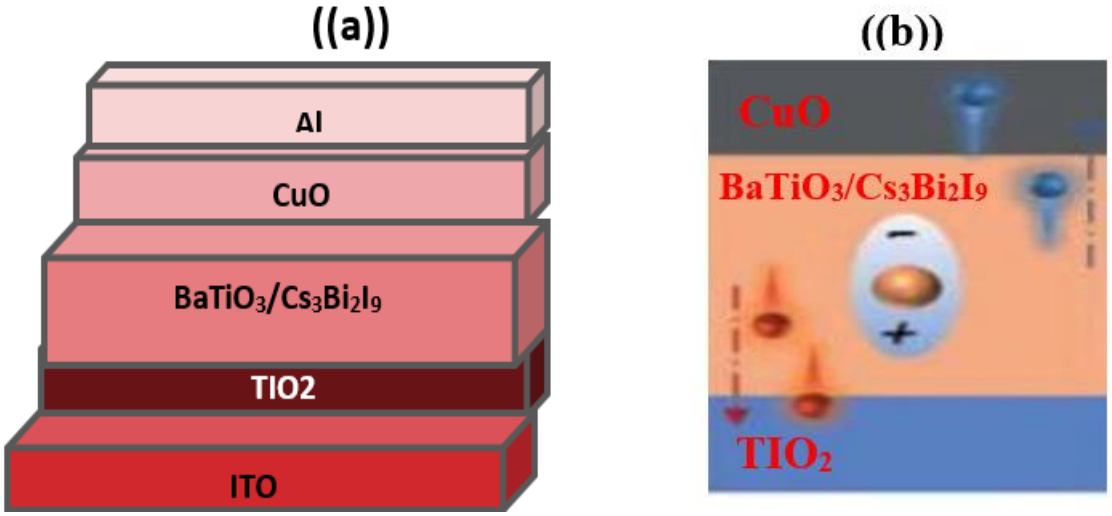

Figure 2. (a) $BaTiO_3/Cs_3Bi_2I_9$ composite film (b) Polarization schematic diagram of the-PSCs

2.5. Measurement and Characterization

X-ray diffraction (XRD, model -6000 Shimadzu Japan) with Cu Kα radiation (λ=1.5406 Å). was used to characterize the size and crystal structure of the sample. Scanning electron microscopy (SEM) was used to characterize the surface morphologies (type – VEGA 3SBU- NO118-0014). Spectroscopy (UV-1800: SHIMADZU) was used to determine the band gap of the samples. The effective area of the cell was defined as 1.5 cm^2. The current density-potential (J-V) curves of prepared PSCs were recorded using Ovometer digital (FLUKE 17B) and decade resistance (model- 8000-England)

3- Results and Discussion

X-ray diffraction analysis is used to identify the crystallinity of the compound as well as the particle size for nano material. The particle size was calculated according to the Scherer relationship as shown in equation 5. [17]

$$L = \frac{k\lambda}{BCos\theta} \quad \text{.....(5)}$$

Where L is nano crystal size, K is constant, λ is the wavelength of radiation in nanometer (λ Cu Kα = 0.15405 nm), θ is the diffracted angle of the peak, β is the full width at half maximum of the peak in radians[8]. Figure 3 displays the XRD pattern of the prepared compounds. The peaks are indexed as $BaTiO_3$ structures (JCPDS: NO.00-039-0536). [18]. The $Cs_3Bi_2I_9$ structure (JCPDS: NO.01-073-0707) [19] and the CuO structure (JCPDS:NO-05-0661) [20]. The compound barium titanate has a nano size range of 55 to 85, but after impregnating with $Cs_3Bi_2I_9$, the results showed a change in size to the range of 25 to 72.

X-ray diffraction shows the nano size of the copper oxide crystal, as well as the absence of additional peaks, indicating the purity of the compound and its freedom from impurities.

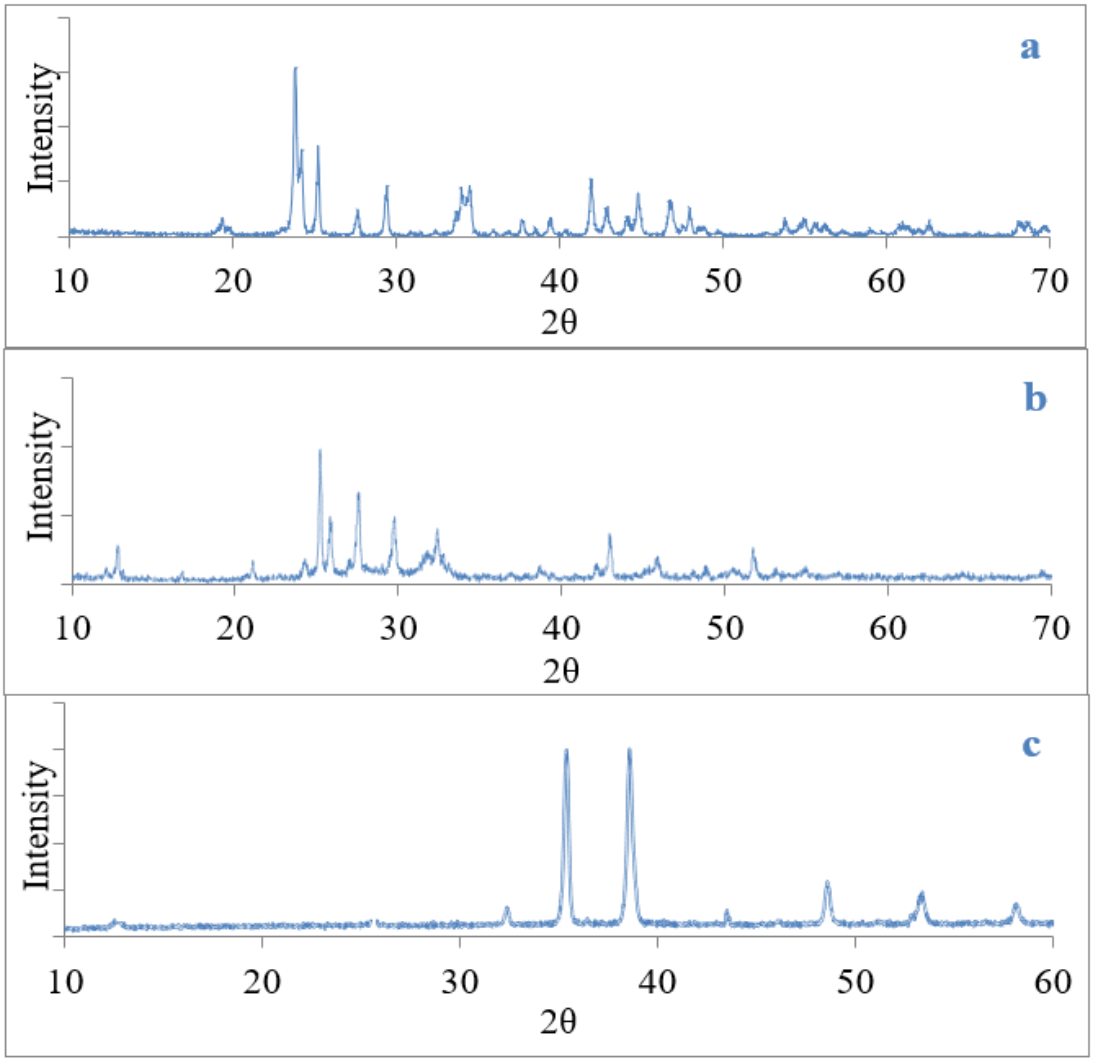

Figure 3. (a) XRD patterns of (a) $BaTiO_3$(b) $BaTiO_3$/ $Cs_3Bi_2I_9$ (c) CuO powder

According to the scanning electron microscope (SEM), the morphology of barium titanate prepared by the hydrothermal method differs greatly from the morphology of barium titanate mixed with perovskite, as shown in figure (4.a), where the surface of $BaTiO_3$ consists of large grains with the appearance of clear voids and the thickness of the layer reaches 51 microns, as shown in figure (4.c), while $BaTiO_3$/$Cs_3Bi_2I_9$ figure (4.b) shows that the surface is transformed to a more homogeneous shape and the nano layer became thinner (18 microns), as shown in figure (4.d).

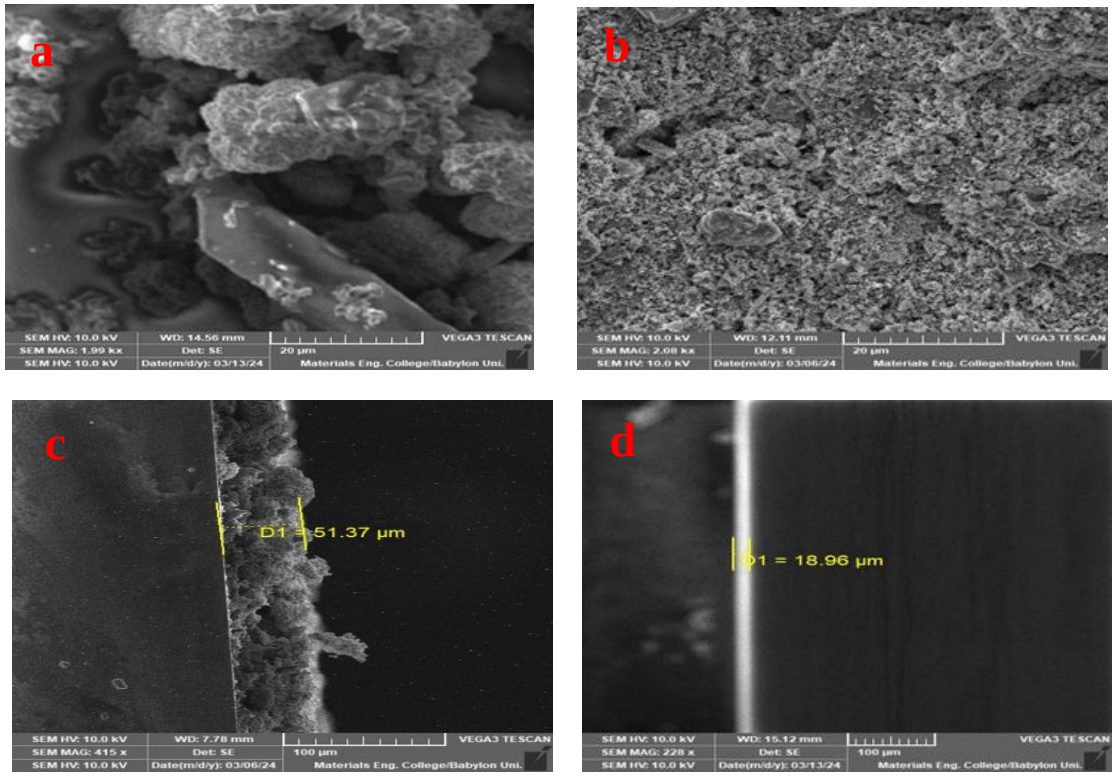

Figure 4. SEM of the surface (a) $BaTiO_3$ (b) $BaTiO_3/Cs_3Bi_2I_9$ thickness of layer of (c) $BaTiO_3$ (d) $BaTiO_3/Cs_3Bi_2I_9$

The optical properties of the prepared $BaTiO_3$ and $BaTiO_3/Cs_3Bi_2I_9$ compounds were measured, and it was found that both were absorbed in the visible region. The absorption peak in Figure 5 changes after mixing. It goes from 300 nm for $BaTiO_3$ (Figure 5.a) to 500 nm for $BaTiO_3/Cs_3Bi_2I_9$ (Figure 5.b). There was also a shift in the energy band gap, which was calculated according to Tauc relationship equation 6. [21] from 3.8 (ev) for $BaTiO_3$ figure (5.c) to 2.8(ev) for $BaTiO_3/Cs_3Bi_2I_9$ figure (5.d).

$(\alpha\lambda\nu)=C(h\nu - Eg)^n$ ……..(6)

Where C is constant , is absorption coefficient , Eg is band gap of compound ,n is depends on the type of transition .The average band gap was determine from the intercept of linear portion of the $(\alpha\lambda\nu)^2$ vs .hv [22]

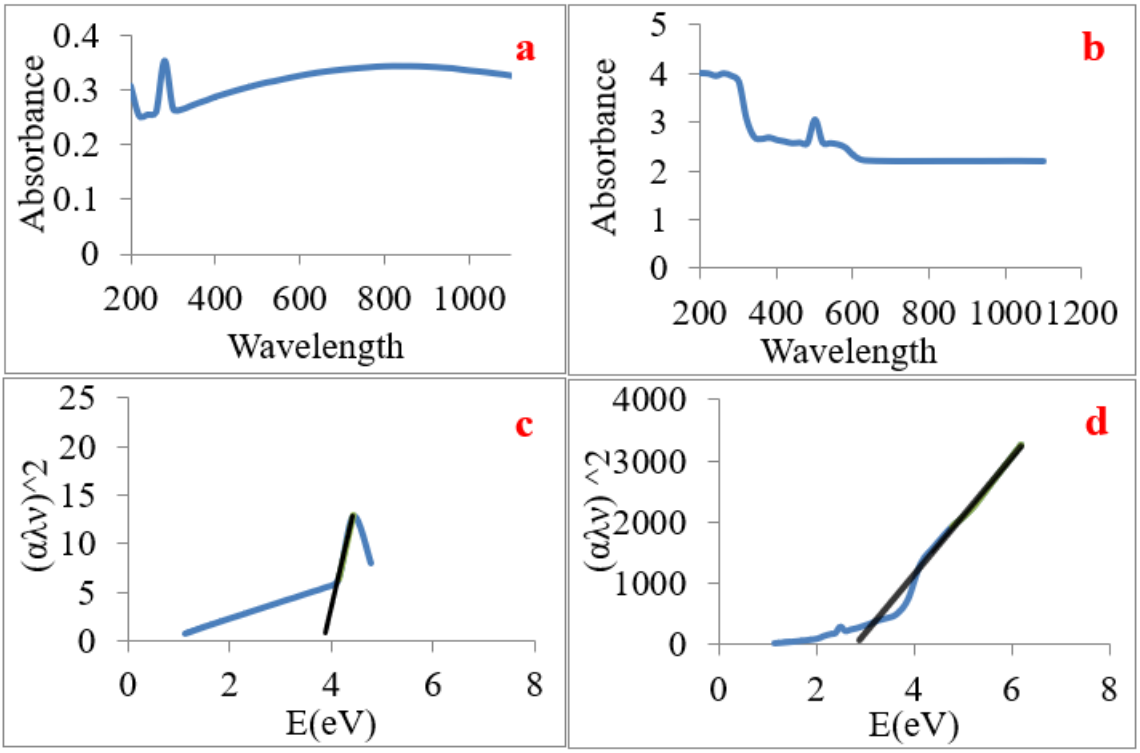

figure 5. UV-vis spectra of (a) $BaTiO_3$, (b) $BaTiO_3/Cs_3Bi_2I_9$. The band gap of $BaTiO_3$ (c), and $BaTiO_3/Cs_3Bi_2I_9$ (d).

Figure 6. and Table 1 show the photovoltaic performance of the solar cell manufactured from mixing barium titanate with perovskite ($BaTiO_3/Cs_3Bi_2I_9$), which gave a photo conversion efficiency (PCE) of 2.4% with a high open-circuit voltage (Voc) of 0.540 V, a short-circuit current (Isc) of 5 mA, and a fill factor (FF) of 0.88. Figure 6.a illustrates the calculation of power against voltage, revealing a value of 2 $mWcm^{-2}$, which figure 6.b confirms.

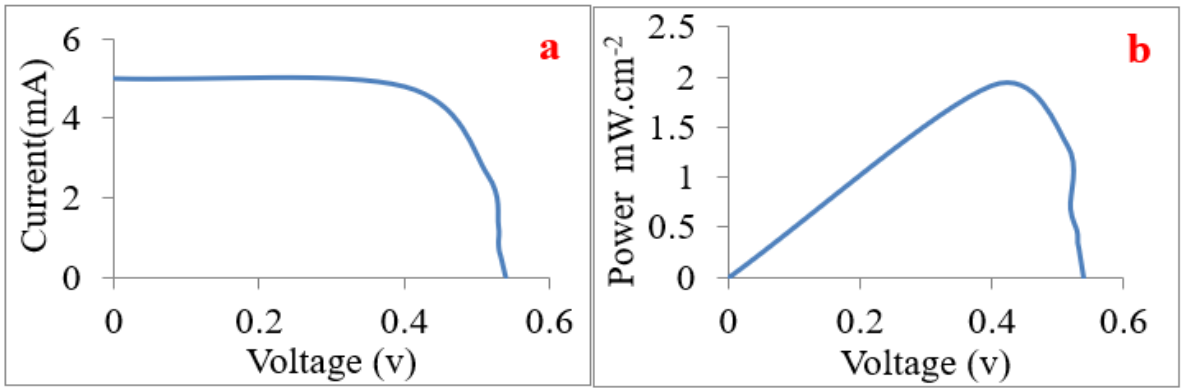

Figure 6. I-V characteristic for $BaTiO_3/Cs_3Bi_2I_9$, for active area 1 cm under light intensity (100 mw/cm^2)

Table 1. Photoelectrical parameters of $BaTiO_3/Cs_3Bi_2I_9$ for active area 1 cm under light intensity (100 mw/cm^2)

MIX	V_{oc} v	I_{sc} mA	FF	ɳ
$BaTiO_3/Cs_3Bi_2I_9$	0.540	5	0.88	2.4

4. Conclusion

In summary, all layers of the solar cell have been prepared using the drip method. These included the titanium oxide layer, the electron-transfer materials (ETMs), the perovskite mixture with barium titanate ($BaTiO_3/Cs_3Bi_2I_9$), and then the copper oxide, the hole-transfer materials (HTMs). This method had an efficiency of up to 2.4%. Furthermore, adding perovskite to the titanate compound resulted in an improvement in its optical properties. The energy band gap was shifted from 3.8 eV to 2.8 eV, and it also led to an improvement in the external shape of the titanate barium in SEM, which affected the increase in the efficiency of its photoelectric performance.

References

[1] Van-Pham D,et al.[2021]: Fabrication of electrospun BaTiO3/chitosan/PVA nanofibers and application for dye-sensitized solar cells, *IOP Conf. Ser. Earth Environ. Sci.*, vol. 947, no. 1, doi: 10.1088/1755-1315/947/1/012017.

[2] Cook G., Billman L., and Adcock R.: Photovoltaic Fundamental, pp. 1–68, 1995.

[3] Dambhare M.V, Butey B, and Moharil S, [2021]:Solar photovoltaic technology: A review of different types of solar cells and its future trends. in Journal of Physics: Conference Series, IOP Publishing Ltd. doi: 10.1088/1742-6596/1913/1/012053.

[4] Khazaal, M., Abbas, Z.K. and Abd Alkathem, Z.H. [2023]: A Review on catalytic Performance for Solid Oxide Cell Components. Journal of Kufa for Chemical Sciences, 3(1), pp.38-54.

[5] Zhang C., Li X., Ding L., Jin C., and Tao H. [2022]: Effect of $BaTiO_3$ powder as an additive in perovskite films on solar cells," *RSC Adv.*, vol. 12, no. 13, pp. 7950–

7960. doi: 10.1039/d1ra09374f.

[6] K. A, T. K, S. Y, and M. T,[2009]:Organometal halide perovskites as visible-light sensitizers for photovoltaic cells. J. Am. Chem. Soc., vol. 131, no. 17, pp. 6050–6051.

[7] Tomaszewski P.E, [1994[:Crystal Structure and Phase Transitions in the A3B2X9 Family of Crystals. Phys. Status Solidi, vol. 181, no. 1, pp. 15–21, doi: 10.1002/pssb.2221810102.

[8] Khazaal, M. H., Staniforth, J. Z., Alfatlawi, Z. A., Ormerod, R. M., & Darton, R. J. [2018]: Enhanced methane reforming activity of a hydrothermally synthesized codoped perovskite catalyst. Energy & fuels, 32(12), 12826-12832.

[9] Ray A.K,[2007]:Synthesis and characterization of BaTiO3 powder prerared by combustion process. M.SC.Thesis, Department of Ceramic Engineering National Institute of Technology Rourkela

[10] Krebs F.C.[2006]:Solar Energy Materials & Solar Cells: Editorial. Sol. Energy Mater. Sol. Cells, vol. 90, no. 10, p. 1363, doi: 10.1016/j

[11] Tripathy S.K, Sahoo T, Mohapatra M, Anand S, and DasR.B, [2005]:XRD studies on hydrothermally synthesised BaTiO 3 from TiO 2 – Ba (OH) 2 – NH 3 system. vol. 59, pp. 3543–3549, 2005, doi: 10.1016/j.

[12] Abd A.N,[2023]:Free-Lead Perovskite Materials , CsFeCl3 And Cs3Fe2Cl9 , In Solar Cell. ACE J. Adv. Res. Phys. Sci. doi: 10.59218/makacejarps.2023.12.19.

[13] Al-Marzouki F.M, Al-Hartomy O.A, and Shah M.A,[2011]:Preparation of copper oxide (CuO) nanoparticles and their bactericidal activity. Int. J. Manuf. Mater. Mech. Eng., vol. 1, no. 4, pp. 58–64, doi: 10.4018/ijmmme.2011100104.

[14] Iannello J.F,[2018]:Perovskite solar cells fabricated via scalable dip coating methods. [Online]. Available: https://rdw.rowan.edu/etd

[15] Basaleh A.S, Mohamed R.M,[2020] Synthesis and characterization of Cu-BaTiO3 nanocomposite for atrazine remediation under visible-light radiation from wastewater. J. Mater. Res. Technol., vol. 9, no. 5, pp. 9550–9558, doi: 10.1016/j.jmrt.2020.06.081.

[16] Arjmand F, FatemiS.J, Maghsoudi.S, and Naeimi A,[2021]:The first and cost

effectivenano-biocomposite, zinc porphyrin/ CuO/reduced graphene oxide, based on Calotropis procera plant for perovskite solar cellas hole-transport layerunderambient conditions. J. Mater. Res. Technol., vol. 16, pp. 1008–1020, doi: 10.1016/j.jmrt.2021.12.012.

[17] Harbbi K.H, and Jahil S.S,[2017]: Study the Lattice Distortion and Particle Size of One Phase of MnO by Using Fourier Analysis of X-ray Diffraction Lines Adv. Phys. Theor. Appl., vol. 65, no. x, pp. 6–22.

[18] Jassim G, Najim N, and Salih W, [2021]:Preparation of Micro Barium Titanate Powder and Comparison with Nano Powder Properties. J. Appl. Sci. Nanotechnol., vol. 1, no. 4, pp. 12–23, doi: 10.53293/jasn.2021.3653.1033.

[19] Park B.W, Philippe B, Zhang X, Rensmo H, Boschloo G, and Johansson E.M.J, [2015]: Bismuth Based Hybrid Perovskites A3Bi2I9 (A: Methylammonium or Cesium) for Solar Cell Application. Adv. Mater., vol. 27, no. 43, pp. 6806–6813, doi: 10.1002/adma.201501978.

[20] Article R, [2016]:A Brief Review on Synthesis and Characterization of Copper Oxide Nanoparticles and its Applications. J. Bioelectron. Nanotechnol., vol. 1, no. 1, pp. 1–9, doi: 10.13188/2475-224x.1000003.

[21] Mehta S.K, Kumar S, Chaudhary S, and Bhasin K.K, [2009]:Supplementary Material (ESI) for Nanoscale Supplementary data Nucleation and growth of surfactant passivated CdS and HgS NPs: Time dependent Absorption and Luminescence profiles. R. Soc. Chem., no. c, pp. 1–6.

[22] Brian D. Viezbicke, Shane Patel, Benjamin E. Davis, and Dunbar P. [2015]: Evaluation of the Tauc Method for Optical Absorption Edge Determination: ZnO Thin Films as a Model System Physica Status Solidi, B, 252, 1700-1710, DOI:10.1002/pssb.201552007.